WIND ENERGY
*Wind Energ.* 2009; **12**:348–362
Published online 30 September 2008 in Wiley Interscience
(www.interscience.wiley.com) DOI: 10.1002/we.297


# The Influence of the Wind Speed Profile on Wind Turbine Performance Measurements

**Rozenn Wagner*, Ioannis Antoniou, Søren M. Pedersen, Michael S. Courtney and Hans E. Jørgensen,** Wind Energy Department, Risø/DTU, Frederiksborgvej 399, Postboks 49, 4000 Roskilde, Denmark

**Key words:**
wind turbine performance; wind shear; profiles; turbulence; BEM simulations; equivalent wind speed

*To identify the influence of wind shear and turbulence on wind turbine performance, flat terrain wind profiles are analysed up to a height of 160 m. The profiles' shapes are found to extend from no shear to high wind shear, and on many occasions, local maxima within the profiles are also observed. Assuming a certain turbine hub height, the profiles with hub-height wind speeds between 6 m $s^{-1}$ and 8 m $s^{-1}$ are normalized at 7 m $s^{-1}$ and grouped to a number of mean shear profiles. The energy in the profiles varies considerably for the same hub-height wind speed. These profiles are then used as input to a Blade Element Momentum model that simulates the Siemens 3.6 MW wind turbine. The analysis is carried out as time series simulations where the electrical power is the primary characterization parameter. The results of the simulations indicate that wind speed measurements at different heights over the swept rotor area would allow the determination of the electrical power as a function of an 'equivalent wind speed' where wind shear and turbulence intensity are taken into account. Electrical power is found to correlate significantly better to the equivalent wind speed than to the single point hub-height wind speed. Copyright © 2008 John Wiley & Sons, Ltd.*

*Received 4 July 2007; Revised 18 August 2008; Accepted 31 August 2008*

## Introduction

As a result of many investigations, it is widely known today that the power curve of a wind turbine depends upon a large number of meteorological and topographic parameters. Wind shear, turbulence and inclined airflow are among the most important parameters that influence the uncertainty of the power curve measurements.[1–7] These parameters also influence the readings of the cup anemometer used to record the wind speed,[8] but this influence will not be addressed in the present paper.

The influence of the meteorological conditions on the mean vertical wind gradient and the turbulence intensity, and the way these factors influence the power performance and hence the annual energy production of the Aeolus II wind turbine, is readily shown in the results of Albers and Hinsch.[3] Kaiser *et al.*[5] try to decrease the uncertainty of site-specific effects on power curves by estimating the influence of turbulence on the turbine's power curve. A common characteristic of these and other efforts is that the effects of wind shear and turbulence have not been evaluated independently. Paulsen[7] performed simulations for different wind shears and turbulence intensities, in order to investigate their relative influence. A major shortcoming of all of the

*Correspondence to: R. Wagner, Wind Energy Department, Risø/DTU, Frederiksborgvej 399, Postboks 49, 4000 Roskilde, Denmark.
E-mail: rozenn.wagner@risoe.dk

studies mentioned above, is that the wind speed has been measured only at hub height or over the lower part of the turbine rotor. Frandsen *et al.*[6] address the shortcomings of the measurement method by suggesting an alternative extended power performance analysis method. The ACCUWIND project introduces the influence of secondary parameters, such as the vertical inflow and the turbulence intensity, in power performance in order to achieve more reliable power curves.[9]

In the latest edition of the international standard for power performance,[10] the wind speed at hub height is the primary input parameter for power curve measurements, with air density as the only other considered parameter. This method suffers from an inherent uncertainty, namely the assumption that the wind speed at hub height is representative of the wind over the whole turbine swept rotor area. While this assumption was probably adequate for smaller wind turbines, the measured results show that this is rarely true for the modern multi-MW ones. With large diameters and high hub heights, large turbines are often exposed to highly varying wind conditions comprising large wind shear, turbulence variations and direction shear within the swept rotor area. As a consequence, considerable deviations often occur between the expected and the produced power when this is given as a function of the hub-height wind speed only.

There is mounting pressure from within the wind energy community for the adoption of a new method that will result in a decrease in the uncertainty of the power performance measurements. A first step in this direction is the use of the wind speed over the whole swept rotor area as an input parameter. Until recently, this would mean the erection and instrumentation of a meteorological mast reaching tip height. Today, the evolution of remote sensing probably allows this measurement to be made with sufficient accuracy with the help of a ground-based instrument.

The goal of this study is to investigate, through simulations, how a more detailed measurement of the wind speed in front of the rotor may reduce the scatter in power curve measurement. In the following, classified wind profiles, derived from measurements, are used as input for a model simulating the wind field and the turbine power output. A method based on an 'equivalent wind speed', taking the wind shear into account, is presented. This method is applied with the model outputs to produce a power curve. Different definitions are suggested, permitting us to also investigate the influence of turbulence intensity and whether the use of a 'true-flux' wind speed through the swept rotor area is advantageous for the more accurate presentation of the turbine's power curve.

## Description of the Test Site Where the Profiles Were Measured

Wind profiles were measured at the Danish National Test Station for Large Wind Turbines, which is situated at Høvsøre in the northwest of Denmark. The test site is flat, surrounded by grassland with no major obstacles and is situated at a distance of 1.7 km from the west coast of Jutland. A row of turbines is aligned in the north-south direction, parallel to the coast with the prevailing wind blowing from the west. Figure 1 shows the site layout and Table I the instruments used. The wind profiles have been collected by combining the measurements from two met masts; the intensively instrumented met mast at the south of the turbines row and the higher aviation light meteorological mast. The distance between the two met masts is 350 m.

## Method Suggested to Account for the Wind Shear in the Power Curve Measurement

The electrical power, $P$, produced by a wind turbine can be expressed as the power available in the wind (energy flux): $\frac{1}{2}\rho AU^3$, where $\rho$ is the air density (assumed constant and equal to 1.225 kg m$^{-3}$ in this inves tigation), $A$ the swept rotor area and $U$ is the horizontal component of the wind speed, times the rotor power coefficient $Cp$

$$P = \frac{1}{2}\rho AU^3 C_P \tag{1}$$



**DOI**: 10.1002/we

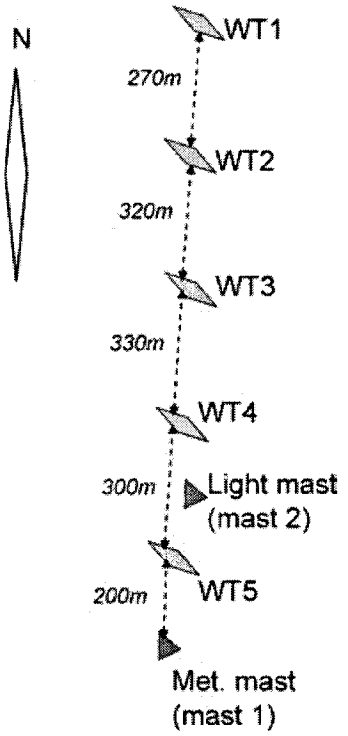


*Figure 1. Sketch of the Danish National Test Station for Large Wind Turbines at Høvsøre 518 × 1062 mm (72 × 72 DPI)*

Table I. Instrumentation of the two met masts at Høvsøre

| Sensor | Position |
|---|---|
| Cup anemometer, boom-mounted on aviation met mast (mast 2) | 165 m |
| Cup anemometer top-mounted (mast 1) | 116.5 m |
| Cup anemometer, wind vane, sonic anemometer, temperature, differential temperature, relative humidity, air pressure (mast 1) | 100 m |
| Cup anemometer, sonic anemometer, differential temperature (mast 1) | 80 m |
| Cup anemometer, sonic anemometer, differential temperature, wind vane (mast 1) | 60 m |
| Cup anemometer, sonic anemometer, differential temperature (mast 1) | 40 m |
| Sonic anemometer (mast 1) | 20 m |
| Cup anemometer, sonic anemometer, differential temperature, wind vane (mast 1) | 10 m |

In order to measure the turbine's power curve in a flat terrain, the wind speed measurements take place using a cup anemometer mounted at hub height and at a recommended distance of 2.5 rotor diameters away from the turbine.[10] The measured electrical power is related to the measured wind speed, averaged over a certain time period, usually 10 min. The wind speed varies with time and its average value is given by the relation

$$\bar{U} = \frac{1}{T}\int_0^T U dt \tag{2}$$

where $T$ is the averaging time period and $U$ is the instantaneous value of the wind speed that can be expressed as a mean and a fluctuating part

$$U = \bar{U} + u, \text{ where } \bar{u} = \frac{1}{T}\int_0^T u dt = 0$$



**DOI**: 10.1002/we

Following de Vries,[11] the average energy flux within the time period $T$ is given by the following relation

$$\begin{aligned}\overline{U^3} &= \overline{(\bar{U}+u)^3} \\ &= \bar{U}^3 + 3\bar{U}^2\cdot\bar{u} + 3\overline{u^2}\cdot\bar{U} + \overline{u^3} \\ &= \bar{U}^3\left(1+3\frac{\overline{u^2}}{\bar{U}^2}+\frac{\overline{u^3}}{\bar{U}^3}\right) \\ &\approx \bar{U}^3\left(1+3\frac{\sigma^2}{\bar{U}^2}\right) \\ &= \bar{U}^3(1+3I^2)\end{aligned} \tag{3}$$

where $\sigma$ is the standard deviation of $U$ and $I$ the turbulence intensity.

Equation (3) takes its final form assuming that the probability distribution for $u$ is symmetrical, in which case $\bar{u}^3$ becomes zero. Although this is not always true, it is a good approximation for neutral conditions. Furthermore, equation (3) shows that, for a given integration interval, the difference between the true average energy flux $\overline{U^3}$ and the energy flux estimated from the average wind velocity $\bar{U}^3$ over the swept rotor area, is a function of the turbulence in the flow.

The effect of turbulence intensity on the turbine power performance is complicated and only partly understood. It depends on the aerodynamics and the inertia of the rotor and the control strategy of the turbine. It can be positive, negative or neutral. A turbine will not always be able to exploit the additional energy arising from the presence of turbulence. For instance, for modern variable pitch/variable speed turbines, this characteristic also depends on the control algorithm.

However, the turbine always responds to changes in the mean wind speed. That the turbine's power curve has traditionally been measured as a function of the mean wind speed at hub height is a convenient simplification based on the assumption that the wind speed at hub height is representative of the wind over the whole swept rotor area. That assumption was acceptable for small wind turbines with low hub height. In practice, wind speed changes within the swept rotor area will influence the power production to a certain degree. Therefore, the measurement of the wind speed at more heights within the swept rotor area gives a better representation of the wind field, and consequently of the incoming energy, than the measurement based only on the hub-height speed.

In the case where the wind speed is known over a number of heights within the swept rotor area, a new parameter, the weighted or 'equivalent' wind speed, is defined by weighting the 10 min average wind speed $\bar{U}_i$ at the corresponding height by the corresponding area ratio $A_i/A$

$$U_{eqM1} = \frac{1}{A}\sum_i \bar{U}_i\cdot A_i \tag{4}$$

where $A_i$ is the area corresponding to the specific data point height and $A$ is the swept rotor area. Figure 2 shows an example for the swept rotor area divided in five segments.

If the turbulence of the flow is accounted for, as in equation (3), the above equation takes the form

$$U_{eqT1} = \frac{1}{A}\sum_i A_i\sqrt[3]{\overline{U_i^3}} \tag{5}$$

Alternatively, the equivalent wind speed can be expressed as the wind speed, which results in the same energy flux through the rotor area as the varying wind speed over the integration period. In this case equation (5) takes the form

$$U_{eqT3} = \sqrt[3]{\frac{1}{A}\left(\sum_i \overline{U_i^3}\cdot A_i\right)} \tag{6}$$



**DOI**: 10.1002/we

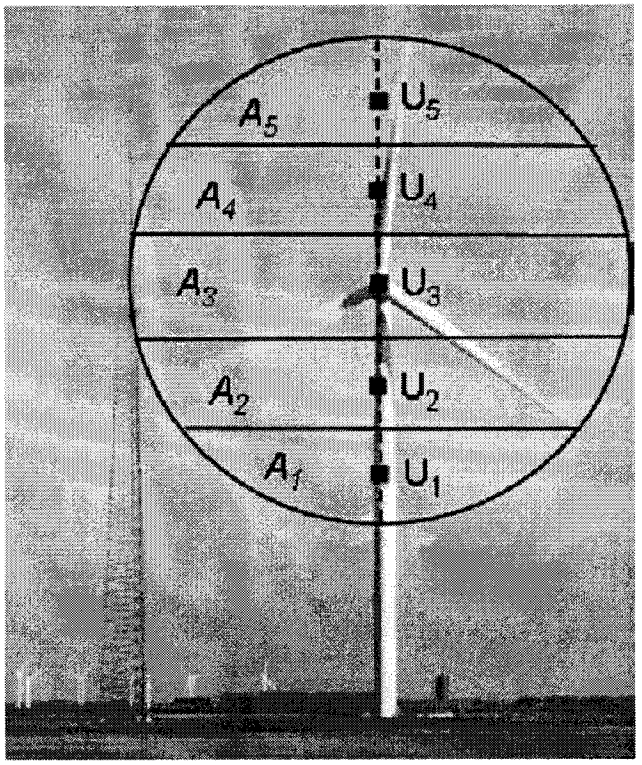


*Figure 2. Swept rotor area of a wind turbine divided into 5 horizontal segments and position of the wind speed 'measurement' 60 × 71 mm (150 × 150 DPI)*

In equations (4) to (6), zero tilt and yaw errors are assumed. In equations (5) and (6), $\overline{U^3}$ is approximated by the last term in equation (3).

## Variations of Measured Wind Profiles in Flat Terrain

The analysis is carried out using data from the met masts at Høvsøre (see Figure 1). For the present analysis, only wind speeds measured with cup anemometers at heights 10, 40, 60, 80, 100, 116 and 165 m are used together with the wind direction. Since the aim of this study is the investigation of the influence of the wind shear on wind turbine performance, a set of differing wind profiles was required. These could have been obtained by using common models such as the logarithmic or the power law profiles. It has been chosen instead to base the profile set on mast measurements since these are more realistic.

The profiles were selected so that they are unaffected by turbine or mast wakes. Profiles from the east were chosen because of their greater diversity. The available measurement heights oblige us to make a linear interpolation between the data points but this does not affect the main purpose of the investigation.

To illustrate the importance of the wind profile as a whole on the power production, Figures 3 and 4 show two examples of wind shear situations. Due to the terrain flatness at Høvsøre, the forms of the wind profiles are mainly determined by the atmospheric stability. Thus, in Figure 3, a situation where the boundary layer is stable during the night (large wind shear) and unstable during the day (well-mixed atmosphere implying very low shear) is shown. In Figure 4, the boundary layer is stable during the whole day (as shown by the gradient below the local maximum) and the wind profile has a local maximum at 80 m height.

The shear situations presented will have different effects on the turbine's power production. For instance, the profiles measured on the 18/01/2006 at 14:00 and the 08/03/2006 at 14:00 look quite different. These



**DOI**: 10.1002/we

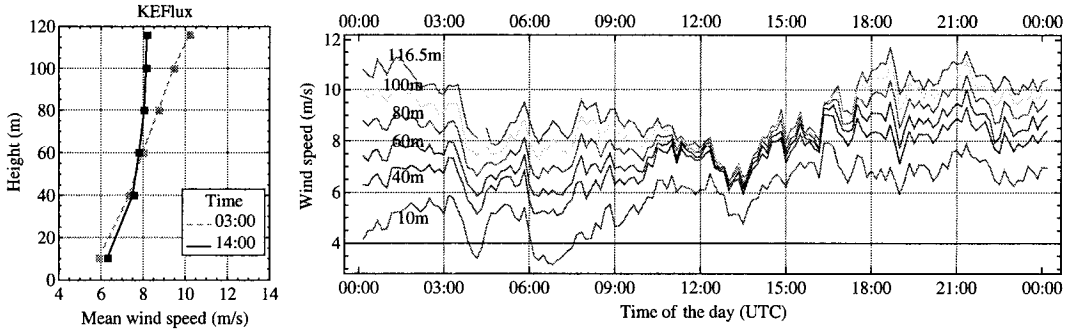


*Figure 3. The wind profile during the 8th of March 2006 236 × 75 mm (600 × 600 DPI)*

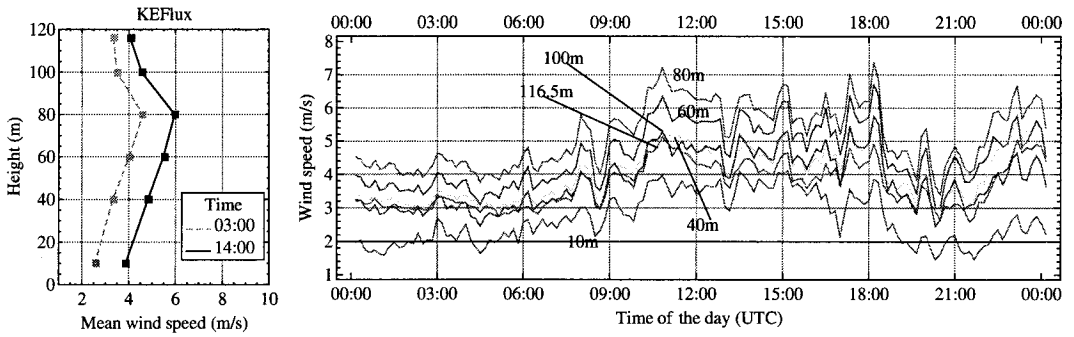


*Figure 4. The wind profile during the 18th of January 2006 236 × 75 mm (600 × 600 DPI)*

profiles are normalized, so they have the same wind speed at 80 m:7 m $s^{-1}$ (see Figure 5), and they are used as input for the simulations of a wind turbine of 107 m rotor diameter. The normalization of the profiles is explained below. The power output from the simulation with the profile presenting a local maxima at 80 m, $P$ = 540 kW, is much lower than the other one, $P$ = 819 kW. This could be misunderstood as an underproduction of the turbine if the power curve is presented as a function of hub-height wind speed only.

In order to study the power performance in the intermediate partial load range that is most relevant for the annual energy production, the wind profiles from 6 to 8 m $s^{-1}$ at a height of 80 m, and for a 1 year period were chosen. Within this period, 2340 profiles were found from the easterly directions between 60 and 120°. These were binned and categorized according to their shape into 173 profiles. Subsequently, all mean profiles were normalized at all heights so that the wind speed at 80 m became equal to 7 m $s^{-1}$, using the ratio $R_i = 7/U_{i80}$, where $i$ is the profile number. This normalization allows us to have the same hub-height wind speed for all the profiles while preserving the profile's shape. It has to be noted that this is done for a small range of wind speeds within the scope of an academic exercise and would not be justified in other circumstances. The same ratio is used to normalize the standard deviations at all heights; in this way, the turbulence intensity at all heights remains the same as in the original profiles.

Figure 6(a) shows how different the profiles can be for a narrow wind speed bin. The 10 most commonly occurring profiles are shown in Figure 6(b), representing 63.6% of all the profiles. It can be observed that for very similar values below hub height, very different profile shapes can be observed above hub height. Therefore, the extrapolation of wind speeds measured below hub height to heights above the hub does not always give a good estimation of the wind profiles over the rotor disc.

Figure 7 shows the distribution of energy flux per unit of the swept rotor area for the 173 profiles mentioned above. The energy flux is defined as $\sum_i \overline{U_i^3} \cdot \frac{A_i}{A}$ where $\overline{U_i^3}$ is approximated as in equation (3),



**DOI**: 10.1002/we

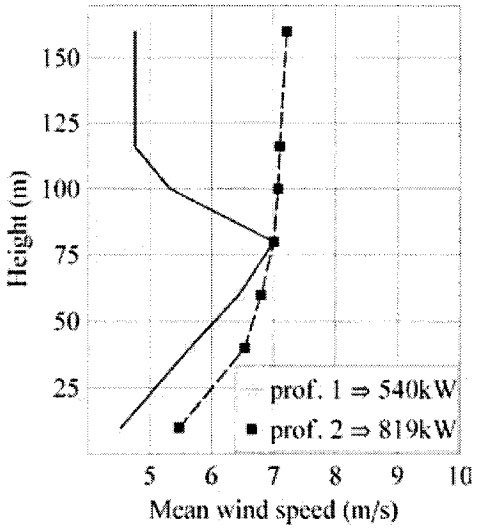


*Figure 5. Profiles normalized to 7 m/s at hub hight, from the measured profiles at 2007-01-18 14:00 and 2006-03-08 14:00. 105 × 127 mm (600 × 600 DPI)*

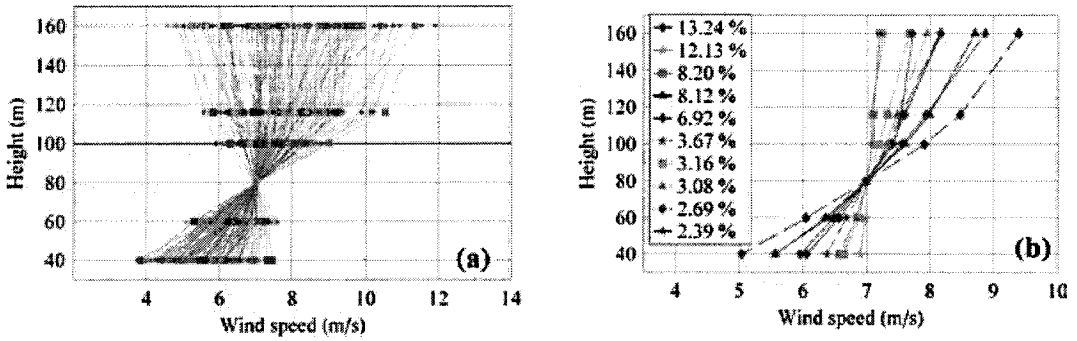


*Figure 6. (a): The classified 173 easterly wind profiles, (b): the 10 most common normalized profiles and their percentage of occurence. 282 × 83 mm (600 × 600 DPI)*

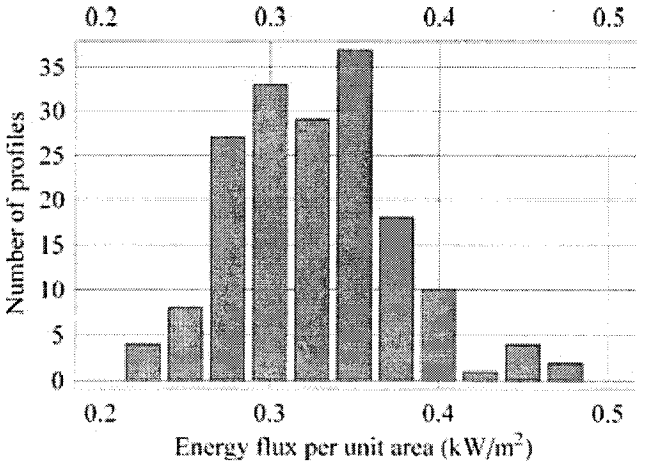


*Figure 7. The energy flux distribution for the 173 normalized easterly wind profiles assuming a wind turbine with a 107 m rotor in diameter and a hub height of 80 m. 141 × 87 mm (600 × 600 DPI)*



**DOI**: 10.1002/we

assuming a wind turbine with a rotor diameter of 107 m. The variation in energy flux is significant, and in fact, according to the distribution, the highest energy flux is twice the magnitude of the lowest one. These large flux variations will also result in significant variations in the electrical power produced by the turbine, the actual magnitude depending on the wind turbine's ability to extract the available energy in the different profile types.

These striking results were only made possible because the wind speed was measured at several heights within the swept rotor area. Note that with a conventional hub-height-only wind speed measurement, the variations in electrical power would be interpreted as uncertainty in the measurement.

## Simulations of the Effect of Wind Profiles on Power Curves

The main objective of this part of the work is to identify the sensitivity of the wind turbine performance to the wind field parameters. Relevant wind field parameters are the mean shear profile, the turbulence shear profile and the tilt and yaw angles. Tilt and yaw angles are not considered in the work presented.

### The Simulation Model and Reference Wind Turbine

A simplified version of the aeroelastic model HAWC2, the AE_N_WIND code, is used in the analysis. It contains the same aerodynamic and wind modules as the full HAWC2 code and can be considered as a Blade Element Momentum model operating in the time domain, thus capable of including turbulence. The main advantage of this simplified version is that its computational time is significantly shorter than the full model.

The sensitivity analysis will be carried out on a model of the Siemens 3.6 MW turbine with a hub height of 90 m and a rotor diameter of 107 m. The simulations' results depend on the aerodynamic model used in the code and the manner in which the induction correction is implemented can have different effects under different situations. Despite this limitation, the results are considered to be generally applicable, as they resemble the results provided by other simulations carried out by Siemens. In the AE_N_WIND simulations, no drive train or generator losses have been included.

The turbine is a variable speed, pitch-regulated turbine: it operates at fixed pitch with a variable rotor speed in the partial load range (optimal Cp tracking). Since the AE_N_WIND code cannot model a turbine controller (it has no generator or pitch degrees of freedom), a fixed rotational rotor speed was used with the relevant speed obtained from a look-up table provided by the turbine manufacturer.

In order to investigate the validity of the constant speed simplification, two power curves—one with fixed speed and one with variable speed—have been calculated with the full HAWC2 model, which includes a turbine algorithm with variable speed. For each of these options, two different shears have been considered: no shear and an extreme shear with a speed-down of 25% at rotor top and bottom. The results are plotted in Figure 8 below for an example where the fixed rotor speed matches the variable rotational speed at 6.5 m $s^{-1}$.

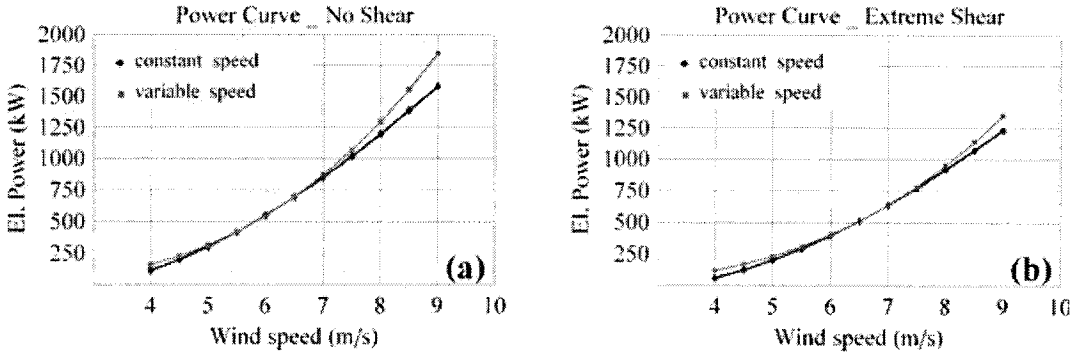


*Figure 8. (a): Calculated power curves with fixed and variable rotational speed. No shear; (b): Calculated power curves with fixed and variable speed. Extreme shear specified. 246 × 76 mm (500 × 500 DPI)*




**DOI**: 10.1002/we

Table II. Equivalent power from outputs from HAWC2 (variable rotational speed) and AE_N_WIND (constant rotational speed) for two different wind fields

| | Power output | |
|---|---|---|
| Wind field | HAWC2 (Variable rpm) | AE_N_WIND (Constant rpm) |
| No shear | 714.9 | 703.2 |
| Extreme shear | 525.3 | 519.7 |
| Ratio | 1.36 | 1.35 |

The resulting power curves have been numerically integrated and weighted with a Gaussian wind speed distribution with a mean value $\mu = 6.5$ m s$^{-1}$ and a standard deviation of $\sigma = 0.65$ m s$^{-1}$ in order to calculate the equivalent power. This equivalent power represents a power value that corresponds to the same accumulated production as if the correct power curve was followed. Due to the curvature of the power curves, the equivalent values are larger than the quasi-steady power value at 6.5 m s$^{-1}$. For larger curvatures, larger power values are seen.

The relative reduction in power between the no shear and the extreme shear cases is found to be very similar for the two different operational strategies (see Table II). As the main objective of this exercise is to look at the relative difference in power output for different wind profiles, it is concluded that the constant RPM speed assumption could be applied.

## *Considered Wind and Turbulence Profiles and the Turbulence Model*

The AE_N_WIND code has the option of user-defined mean wind and turbulence profiles, so that the wind speed and turbulence variations with height are taken into account. In order to validate the user-defined mean and turbulence shear implementation, a number of simulations with simplified input parameters have been carried out (not presented here).

The inputs to the model are the 10 min mean wind speed and standard deviation at 7 heights for each of the 173 normalized profiles (see Section 4). From these, the model generates 10 min time series (with a sample period of 0.2 s) of free wind in a vertical plane of 120 × 120 m$^2$. The Mann model of turbulence[12] is used to simulate the wind fluctuations that are added to the mean wind speed. Wind fluctuations were simulated over a flat terrain and the spectral tensor was calculated with the following parameters: $\alpha\varepsilon^{2/3} = 0.18$ m$^{4/3}$ s$^{-2}$ (where $\varepsilon$ is the viscous dissipation of turbulence kinetic energy), the length scale L = 29.4 m and $\Gamma = 3.9$, this latter parameter being the eddy life time coefficient in the Mann turbulence model.

Figure 9 displays results for one simulation with a power law wind profile with a shear exponent of 0.1, a wind speed of 7 m s$^{-1}$ at 90 m and a turbulence intensity of 10%. It shows the mean wind profiles (left) and the turbulence intensity profiles (right) for different horizontal positions ($y$) in the rotor plane. This illustrates a significant variation of the wind statistical variables across the swept rotor area. Therefore a certain number of simulations are required in order to map the statistical variation in normal turbulence fields expected over a turbine rotor. As in the Mann model, turbulence followed a normal distribution, the sampling distribution of the sample mean: $\langle u(t)\rangle = \frac{1}{N}\sum_{j=1}^{N} u_j(t)$, where $N$ is the number of independent observations, is also normally distributed.[13] Consequently, the variance of the sampling distribution of the sampling mean is: $\sigma^2_{\langle u\rangle} = \frac{\sigma_u^2}{N}$. On this background, 10 simulations for each mean wind profile were decided to be adequate since they reduce the variance of the sampling distribution by 10.



**DOI**: 10.1002/we

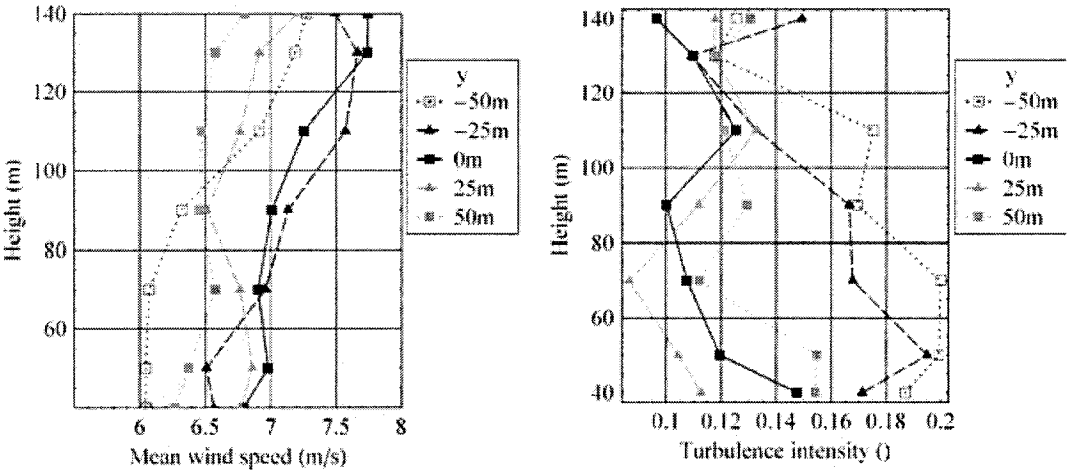


*Figure 9. Large statistical spread of the mean wind speed and the turbulence intensity for one 600 seconds simulation over a 107 m rotor diameter. A power law shear was specified for the mean wind profile. As a consequence of this large statistical spread, it has been decided to run 10 simulations for each profile. 246 × 117 mm (500 × 500 DPI)*

Table III. Summary of the configurations and equivalent wind speed definitions examined. The checked cases are those presented in this paper

| Configuration | $U_{eqM1}$ | $U_{eqT1}$ | $U_{eqT3}$ | $U_{eqL1}$ |
|---|---|---|---|---|
| 1 point at hub height | ✓ | | | ✓ |
| 3 points profile | ✓ | | | ✓ |
| 5 points profile | ✓ | ✓ | ✓ | ✓ |
| 1 circle (at 85% radius) | ✓ | ✓ | ✓ | |
| 2 circles (at 45 and 85% radius) | ✓ | ✓ | ✓ | |

## *Equivalent Wind Speeds Computed from the Simulations*

The main outputs are 10 min time series of the power produced by the turbine, as well as the time series of the free wind at given points in the rotor plane. These points are chosen in two different ways. First, 1, 3 or 5 points are taken within the rotor disc along a vertical line passing through the centre of the rotor, respectively, at hub height (90 m) and at symmetrical positions above and below. Figure 2 illustrates the case of 5 points. The data point height is located at the average height of the segment. In the results and discussions, these configurations are referred to as, respectively, 1-point, 3-point and 5-point configurations.

Secondly, points are taken equally distributed on two circles concentric with the rotor and at radii 45 and 85% of the blade length. This configuration can be seen as a preliminary investigation of measurements made by a turbine-mounted device capable of measuring the free wind on a circular path.

The times series obtained by all these sets of data are used to calculate the equivalent wind speeds defined in Section 3. In the following part, the 10 min average power is plotted as a function of these different wind speeds and compared.

As recapitulated in Table III, these five configurations are used to calculate any of the three equivalent wind speeds; the checked cases are those that are presented in Section 6. Note that in order to look at the influence of the turbulence, some simulations are carried out for laminar flow. In that case, $\bar{U}_i = U_i$ and $U_{eqM1}$ is renamed $U_{eqL1}$.



**DOI**: 10.1002/we

## Comparison of Results for Different Equivalent Wind Speeds

### 1-, 3- and 5-point Profiles

In Figure 10 below, the turbine's power curve and the power coefficient are presented for the cases as described above. For 1-point profiles, we take the wind speed at hub height, which for the case of the normalized profiles is equal to 7 m $s^{-1}$. For the multi-point profiles, the resulting wind speeds are the weighted results using equations (4) to (6). Therefore, in Figures 10 and 11, the wind speed on the horizontal axis corresponds to hub-height wind speed or one of the equivalent wind speeds according to the case.

The lines in the figures of the power curves and the power coefficients represent the polynomial fits of the power curve points calculated using no shear profiles and laminar or turbulent flow as input to the AE_N_WIND code at the corresponding wind speeds. In the case of turbulent flow, the user-defined input standard deviation corresponds to an average value of the standard deviation measured for the different profiles.

The results of the simulations show clearly that by increasing the number of measurement points over a given profile, a less ambiguous relation between the electrical power and the wind speed is obtained [see Figure 10(a)–(d)]. Among the equivalent wind speeds used, the weighted mean wind speed expression [$U_{eqM1}$; equation (4)] represents, for a given number of points, the best approximation to the turbine's power curve, relative to the remaining equivalent wind speed definitions [see Figure 10(e)–(f)]. When accounting for the turbulence in the flow [$U_{eqT1}$; equation (5)], it is expected that the influence of the turbulence will depend on the shape of the power curve and whether it is convex or concave at the specific wind speed interval. In the case where the wind speed is defined in terms of a wind speed resulting in the same energy flux over the swept rotor area [$U_{eqT3}$; equation (6)], the correlation between the equivalent wind and the electrical power, Figure 10(g),(h), is poorer than the ones obtained with the other equivalent speed definitions. In the case of the flat profile, the equations (5) and (6) practically coincide, the only difference being due to turbulence. Hence the deviation observed confirms that the rotor as modeled is less efficient at extracting energy in the presence of wind shear. However, these results are specific for the controller used in these simulations: constant rotor speed and constant pitch. A variable rotation speed would optimize the energy extraction from the wind, and therefore, a higher Cp could be expected. However, this deviation would be minor compared with the deviation due to the wind shear.

In Figure 12, the root mean square of the difference between the simulation results for all wind profiles and the polynomial fit of the no shear power curve, are compared as a function of the configuration. In practice, this is a goodness-of-fit test that shows that by increasing the number of measurement heights in the profile, a better correlation is achieved.

### One and Two Circles Concentric with the Rotor

As mentioned above, in the case of the circle configurations, the wind speed output is given on two circles of radii 45 and 85% of the blade. In order to calculate an equivalent wind speed, the turbine swept rotor area is divided into horizontal segments as we described previously (see Figure 2). The wind speeds at points within the same segment are clustered together and averaged. Finally, these average values are introduced in equations (4) to (6) as $U_i$ ($i$: 1–10).

Figure 11(a)–(d) displays the results obtained with a swept rotor area divided in 10 horizontal segments. As for the profiles' configuration, the results obtained with $U_{eqT1}$ are very close to those obtained with $U_{eqM1}$, so in order to make the figure clearer, the results for $U_{eqT1}$ are not shown in Figure 11. The configuration including wind speed from 45% of the blade (increasing the number of points in each segment) improves the agreement with the no shear power curve (Figure 13).

## Discussion

The shear profiles over a flat terrain were investigated with the help of meterological mast measurements in the interval between 6–8 m $s^{-1}$. The profiles were found to deviate considerably from the logarithmic or the



**DOI**: 10.1002/we

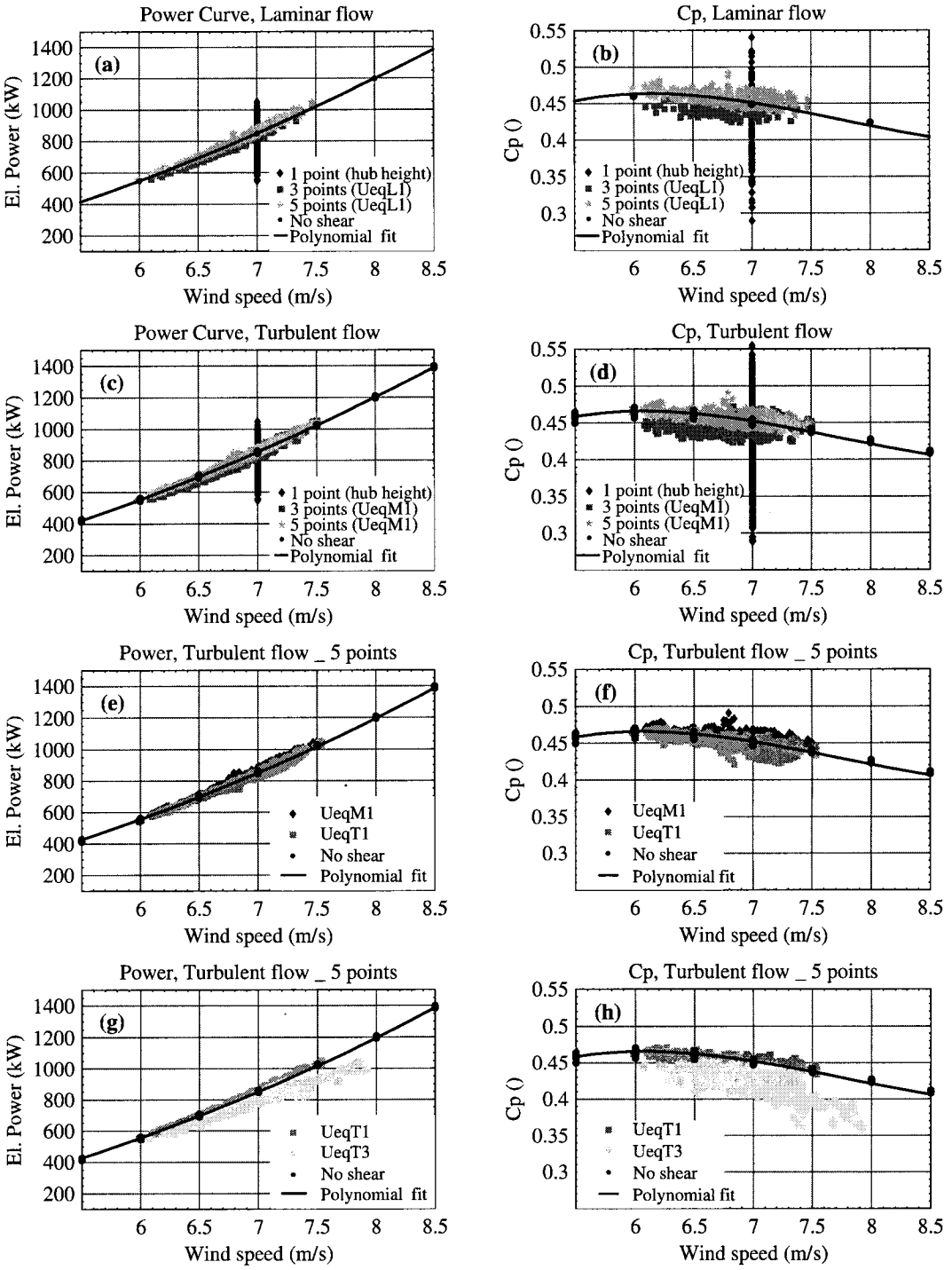


*Figure 10. The power curve and power coefficient as functions of the equivalent wind speeds. (a),(b): comparison between three configurations with laminar flow; (c),(d): comparison between three configurations with turbulent flow; (e), (f): comparison between UeqT1 and UeqM1 expressions for the 5 point configuration; (g), (h): comparison between UeqT1 and UeqT3 expressions for the 5 point configuration. 246 × 311 mm (600 × 600 DPI)*




**DOI**: 10.1002/we

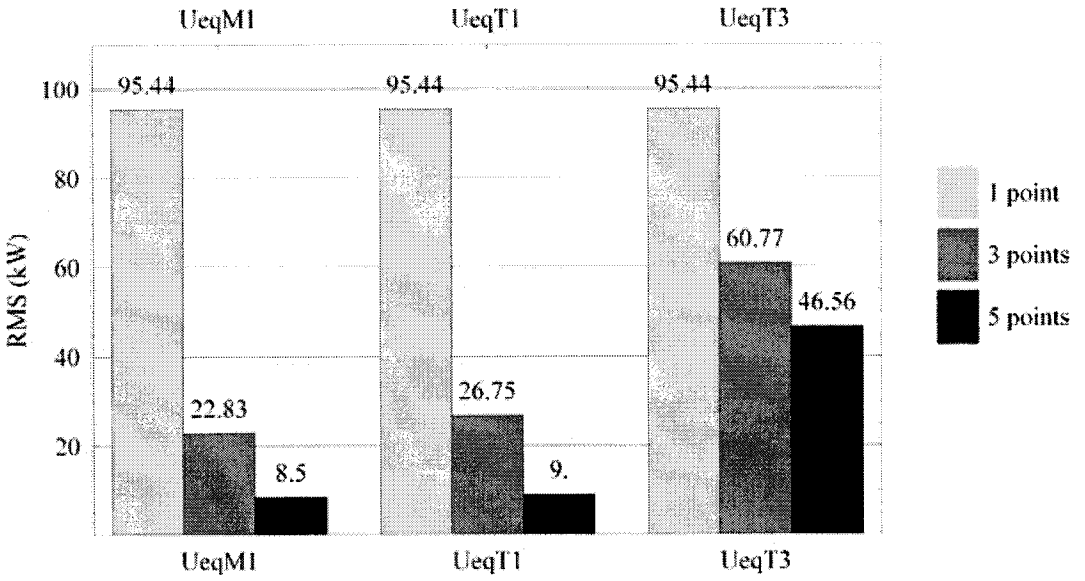


*Figure 11. Comparison of the RMS of the difference between the power from the different profile configurations and the no shear power curve with turbulence using the different equivalent wind speed definitions. 282 × 139 mm (600 × 600 DPI)*

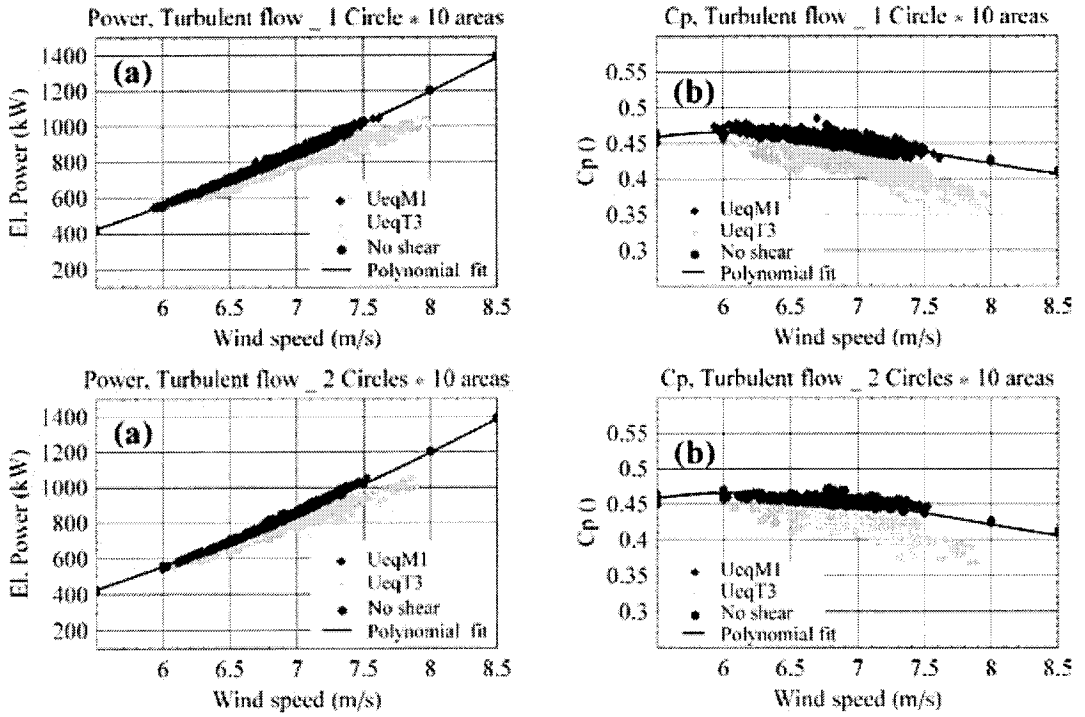


*Figure 12. The power curve and power coefficient as functions of the weighted wind speeds for two different configurations. Comparison of the equivalent wind speeds (a),(b): for a one circle configuration; (c),(d): for a two circles configuration. 246 × 154 mm (500 × 500 DPI)*




**DOI**: 10.1002/we

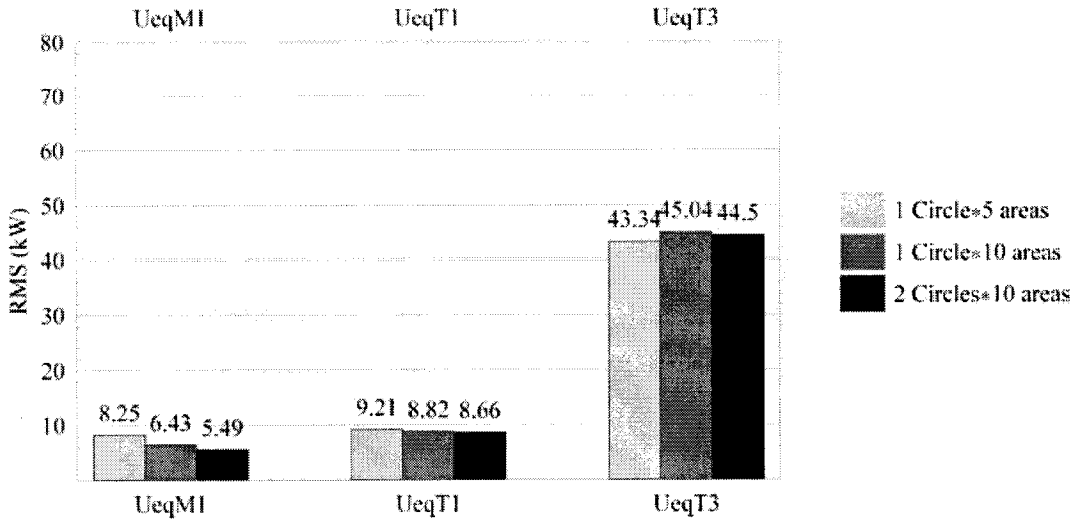


*Figure 13. Comparison of the RMS of the difference between the power from the different circles configurations and the no shear power curve with turbulence using the different equivalent wind speed definitions. 282 × 134 mm (600 × 600 DPI)*

power law profile, which is, as a rule, assumed for power curve simulations. On some occasions, local speed maxima are observed within the measured heights. This is not an unusual situation; such profiles have been observed before at other locations under stable conditions.[14]

Even more important, it was found that the correlation between the electrical power and the wind speed improved as the electrical power was plotted as a function of a weighted wind speed measured at more points on the vertical over the turbine swept rotor area. These initial findings are substantial; however, more work is needed, both in terms of measurements and simulations, at more wind speed intervals, in order to confirm the tendencies observed. The work should also include the influence of parameters like wind direction and turbulence variations as well as the coherence across the swept rotor area.

A reduction in the scatter of the power curve measurements seems probable if the wind speed measurement takes place over the whole rotor height and is not restricted to hub height. The limitations of a 1-point speed measurement increase with the size of the wind turbines and the fact that the hub-height wind speed can no longer be considered as representative of the wind over the whole swept rotor area. Such measurements can take place either using met masts exceeding hub height or by using well–calibrated, ground-based remote sensing instruments like LiDAR and SoDAR[15] placed in front of the turbine. At the same time, the results underline the need for revising the relevant international measurement standards on power curve and site calibration measurements.

The results from the circle configuration simulations also show that it is, in principle, possible to use turbine-mounted, concentrically sensing instruments in order to measure the wind speed over the whole swept rotor area. The scatter in the power curve plot for this case is comparable to the profile measurements. This configuration might be seen as a preliminary investigation of what could be measured by a blade mounted five-hole pitot tube or a nacelle-mounted LiDAR scanning upwind. The pitot tube would provide a complete wind vector at any position within the circle(s). However, this vector would be the apparent wind speed at the airfoil including tangential blade speed and axial induction, whereas the power curve is defined in terms of the upwind free wind speed [the simulations gave us the ('virtual') free wind speed at the rotor plane]. Therefore, a method to calculate and correct for the rotor induction would be necessary. A nacelle-mounted LiDAR would directly measure the free wind in front of the rotor without requiring an induction correction. However, we need to further investigate how measurements from a conically scanning, forward-looking LiDAR could be interpreted for use in power curve measurements.



**DOI**: 10.1002/we

## Conclusions

Large variations have been observed in the wind profiles over a flat site. The results show that the profiles usually do not follow the logarithmic law; instead, their shape, in the case of flat terrain, heavily depends upon the atmospheric conditions. These profiles were used as input to a sensitivity analysis concerning the power production as a function of a weighted ('equivalent') wind speed over the whole swept rotor area as compared with the results of the wind speed only at hub height.

The results from the simulations indicate that measuring the wind speed at an increased number of points over the whole swept rotor area profile, would improve the correlation between wind input and power output. These results support the necessity for the introduction of a new definition for power performance measurements using a distributed measurement of the wind over the swept rotor area instead of using only the hub-height wind speed.

## Acknowledgements

The authors acknowledge the financial support of the Danish Energy Agency to the IMPER project (journal no.: 3302–0106), which made this investigation possible. Siemens Wind Power provided the data for the modelling. The authors gratefully acknowledge the many discussions and useful advice from many, including Uwe Paulsen[1], Helge A. Madsen[1], Kenneth Thomsen[2], Peder Enevoldsen[2] and Leo Thesbjerg[3]. Rozenn Wagner is supported by the Marie Curie ModObs Network MRTN-CT-2006-019369.
[1]Risø/DTU; [2]Siemens Wind Power; [3]Vestas Wind Systems A/S.

## References

1. Antoniou I, Mouzakis F, Albers A, Follrichs U, Curvers T, Verhoef H, Enevoldsen P, Højstrup J, Christensen LC. Identification of variables for site calibration and power curve assessment in complex terrain, project jor3-ct98-0257. *EWEC*, Copenhagen, 2001; 17–22.
2. Dekker JWM, Pierik JTG (eds). *European Wind Turbine Standards II, Project Results. ECN-C-99-073.* Joule III EU Contract JOR3-CT95-0064, June 1998.
3. Albers A, Hinsch C. Influence of different meteorological conditions on the power performance of large WEC's. *DEWI Magazin* 1996; **9**:40–49.
4. Pedersen TF. On wind turbine power performance measurements at inclined airflow. *Wind Energy* 2004; **7**:163–176.
5. Kaiser K, Hohlen H, Langreder W. Turbulence correction for power curves. *EWEC* 2003, Madrid.
6. Frandsen S, Antoniou I, Hansen JC, Kristensen L, Madsen HA. Redefinition power curve for more accurate performance assessment of wind farms. *Wind Energy* 2000; **3**:81–111.
7. Paulsen US, Pedersen TF, Jørgensen HE. Sea–land interaction influence on wind turbine power performance. *EGU* 2006, Vienna.
8. Albers A, Klug H. Open field cup anemometry. *EWEC* 2001, Copenhagen; 276–279.
9. Eecen PJ, Mouzakis F, Cuerva A. Accuwind Work Package 3 Final Report. ECN-C—06-047, CE contract NNE5-2001-00831, May 2006.
10. IEC61400-12-1. Wind turbines-Part 12-1: power performance measurements of electricity producing wind turbines. 2005.
11. Vries, de, O. Fluid dynamic aspects of wind energy conversion, AGARD-AG-243, 1978.
12. Mann J. Wind field simulation. *Probabilistic Engineering Mechanics* 1998; **13**:269–282.; 13
13. Bendat JS, Piersol AG. *Random data: analysis and measurement procedures* (3rd edn). Wiley Interscience: New York, 2000.
14. Antoniou I, Jørgensen HE, Mikkelsen T, Frandsen S, Barthelmie R, Perstrup C, Hurtig M. Offshore wind profile measurements from remote sensing instruments. *EWEC* 2006, Athens.
15. Antoniou I, Jørgensen HE, Mikkelsen T, Pedersen TF, Warmbier G, Smith D. Comparison of wind speed and power curve measurements using a cup anemometer, a LIDAR and a SODAR. *EWEC* 2004, London.